Inorganic Chemistry

Article

pubs.acs.org/IC

Copper-, Palladium-, and Platinum-Containing Complexes of an Asymmetric Dinucleating Ligand

Mohammad Reza Halvagar, Benjamin Neisen, and William B. Tolman*

Department of Chemistry and Center for Metals in Biocatalysis, University of Minnesota, 207 Pleasant Street SE, Minneapolis, Minnesota 55455, United States

Supporting Information

ABSTRACT: The coordination chemistry of an asymmetric dinucleating hexadentate ligand LH_2 comprising neutral alkyltriamine and potentially dianionic dicarboxamido-pyridyl donor sets with copper, palladium, and platinum has been explored. Monometallic, dicopper, and heterodinuclear Cu−Pd and −Pt complexes have been prepared and characterized, including by NMR, EPR, UV−vis, and IR spectroscopy and X-ray crystallography. For example, the monometallic complexes $[(LH_2)MCl]X$ (M = Cu, X = OTf; M = Pd or Pt, X = Cl) were prepared, wherein the metal(II) ions are coordinated to the triamine portion and the pyridyldicarboxamide is unperturbed. Treatment of LH_2 with $[MesCu]_x$ (Mes = mesityl) provided a monocopper(I) complex, again with the metal coordinated only to the trialkylamine donor set. Reaction of $[(LH_2)CuCl]OTf$ with NaOMe resulted in an unexpected migration of the copper(II)−chloride fragment to the pyridyldicarboxamide site to yield $Na[LCuCl]$, from which a dicopper complex LCu_2Cl_2 and mixed-metal complexes LCu(Cl)M(Cl) (M = Pd, Pt) were prepared by addition of $CuCl_2$ or MCl_2, respectively. The heterodinuclear complexes were also prepared by addition of $CuCl_2$ to $[(LH_2)MCl]Cl$.

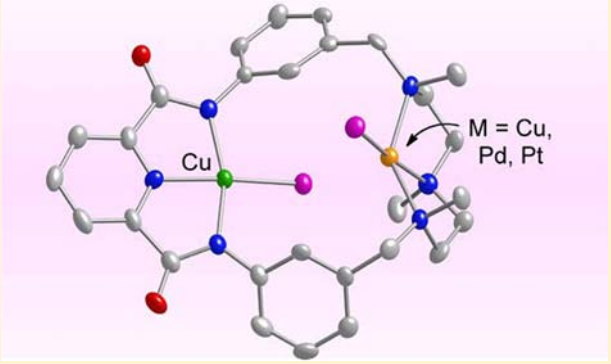

Many dimetallic protein active sites and catalysts contain different metal ions (cf. FeZn purple acid phosphatases,[1] CuZn superoxide dismutase,[2] FeCu cytochrome *c* oxidase,[3] Pd/Cu oxidation catalysts[4]) or two of the same metal ions in different coordination environments and/or oxidation states (cf. dopamine β-monooxygenase, peptidylglycine α-hydroxylating monoxygenase[5]). In efforts to understand the structural and functional properties of such active sites and catalysts, heterodinuclear or otherwise asymmetric complexes are important targets for preparation and characterization.[6] A particularly effective strategy for their synthesis (among others[7]) is to use dinucleating ligands featuring disparate metal binding sites.[8,9] We aim to use this strategy to prepare mixed-valent dicopper and heterodinuclear complexes containing copper adjacent to other metal ions, with the ultimate goal of designing new oxidation catalysts and gaining new mechanistic insights into oxidation catalysis.

A recent report[9c] of NiFe models of a key portion of the active site of carbon monoxide dehydrogenase using LH_2 (Figure 1) as a supporting ligand inspired us to explore its copper coordination chemistry. A key objective is to prepare molecules with reactive cores like **1** and **2**, which have been considered[10,11] as the active oxidant in particulate methane monoxygenase.[12] Such species are of great interest due to their novelty and the significance of the hydrocarbon functionalization reaction they are proposed to perform. The ligand LH_2 is attractive for use in preparing such species because it features two distinct donor arrays within a single macrocyclic ligand framework, a potentially dianionic, meridional pyridyldicarboxamide, and a neutral, flexible trialkyltriamine. Both donor sets have been used in isolation to examine copper chemistry relevant to oxidation catalysis by copper sites in enzymes. For example, the pyridyldicarboxamide **3** was found to stabilize a copper(III)−hydroxide complex that rapidly abstracts hydrogen atoms from weak C−H bonds,[13] and was used to prepare a tetragonal copper(II)-superoxide complex.[14] Trialkyltriamine ligands have been used extensively to support $Cu(I)/O_2$ chemistry, including for the isolation and characterization of a variety of reactive intermediates, such as peroxodicopper and bis(oxo)dicopper(III,III) complexes.[15] We envisioned that

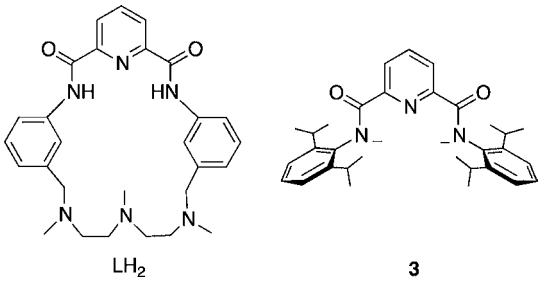

Figure 1. Ligand LH_2 and related pyridyldicarboxamide **3**.

Received: September 1, 2012
Published: December 26, 2012

   dx.doi.org/10.1021/ic301914u | *Inorg. Chem.* 2013, 52, 793−799

insertion of copper ions into LH_2 could provide novel dicopper species with proximal metal ions in coordination environments that differ significantly with respect to geometry and charge, resulting in unique reactivity.

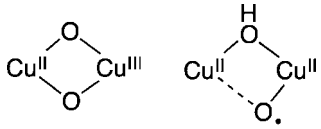

1 2

In addition, heterobimetallic complexes containing copper ions adjacent to other metal ions could be accessible using LH_2, if sequential incorporation of the different metal ions could be implemented. Mixed Pd- or Pt/Cu systems are of particular interest in the context of the Wacker and related oxidation processes,[4] where, for instance, the role of Cu in the Pd-catalyzed oxidation of olefins continues to be debated.[16,17] New types of heterobinuclear Pd- and Pt/Cu complexes[16,18] would be useful for probing mechanistic issues surrounding oxidation catalysis,[19,20] with LH_2 being particularly advantageous in view of recent studies of Pd complexes supported by multidentate alkylamine ligands.[21−24]

Herein, we report our initial explorations of the coordination chemistry of LH_2 with copper, palladium, and platinum ions. A variety of mono- and dimetallic complexes of these metal ions have been prepared and characterized, and migration of copper(II) from one donor site to the other has been observed. These synthetic and structural studies demonstrate the versatility of LH_2 as a supporting ligand for generating asymmetric dinuclear complexes comprising copper, palladium, and/or platinum ions, and provide a foundation for future reactivity and mechanistic work.[25]

RESULTS AND DISCUSSION

Synthesis and Characterization of LH_2 and Cu/Pd, Pt−Chloride Complexes. We prepared and stored LH_2 as its hydrochloride salt as described in the literature, except using a different method for a key reduction step that in our hands was more reliable than the published[9c] procedure (see Experimental Section). Treatment of LH_2·2HCl with base followed by $Cu(OTf)_2$ yielded the monometallated complex **4** (Scheme 1), which was isolated as a blue solid. The formulation of **4** was confirmed by ESI-MS, EPR spectroscopy, and X-ray crystallography. In the ESI mass spectrum obtained for a solution of the complex in MeOH, a parent ion at m/z 584 was observed with an isotope pattern consistent with the presence of a single copper ion (Figure S1). The EPR spectrum exhibits a slightly rhombically distorted axial signal consistent with an isolated N-donor ligated Cu(II) center in a tetragonal coordination environment, but with N-superhyperfine coupling unresolved (Figure 2a,b; g_x = 2.170, g_y = 2.054, g_z = 2.034, $A_{\|}$(Cu) = 192 × 10^{-4} cm^{-1}). Confirmation of the insertion of a single Cu(II) ion into the trialkylamine portion of LH_2 came from its X-ray crystal structure (Figure 3a). The metal ion adopts a coordination geometry slightly distorted from square planar, and exhibits metal−ligand bond distances typical for 4-coordinate Cu(II) (Table 1).

Treatment of LH_2·2HCl with excess $[MesCu]_x$ (Mes = mesityl) also yielded a mononuclear complex (**5**), in this case comprising a single Cu(I) ion. In addition to exhibiting a ^{1}H NMR spectrum consistent with its formulation (Figure S2), the ESI mass spectrum of **5** contained a parent ion isotope pattern

Scheme 1

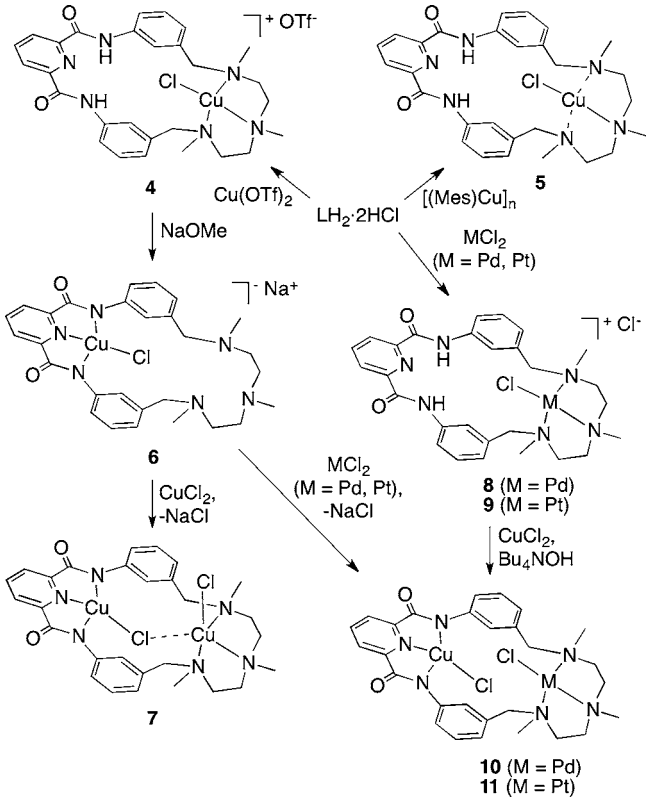

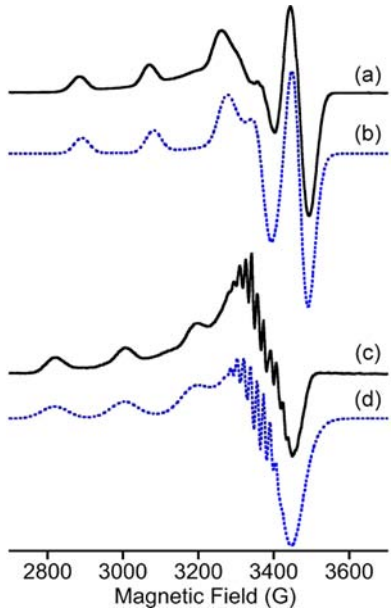

Figure 2. EPR spectra of **4** (a) and **6** (c) with simulations (b and d, respectively). Conditions: 9.64 GHz, 2 K. See text for parameters determined from the simulations.

identical to that of **4** (Figure S3), indicating that it contains one copper ion and a chloride (apparently derived from the starting HCl salt of the ligand). The X-ray structure of **5** (Figure 3b) also is similar to that of the cationic portion of **4** insofar as it shows a copper−chloride moiety coordinated to the trialkylamine site but no metal ion bound to the pyridyldicarboxamide portion of the ligand. Unlike **4**, however, the metal ion in **5** is bound strongly to only one nitrogen donor from the

dx.doi.org/10.1021/ic301914u | Inorg. Chem. 2013, 52, 793−799

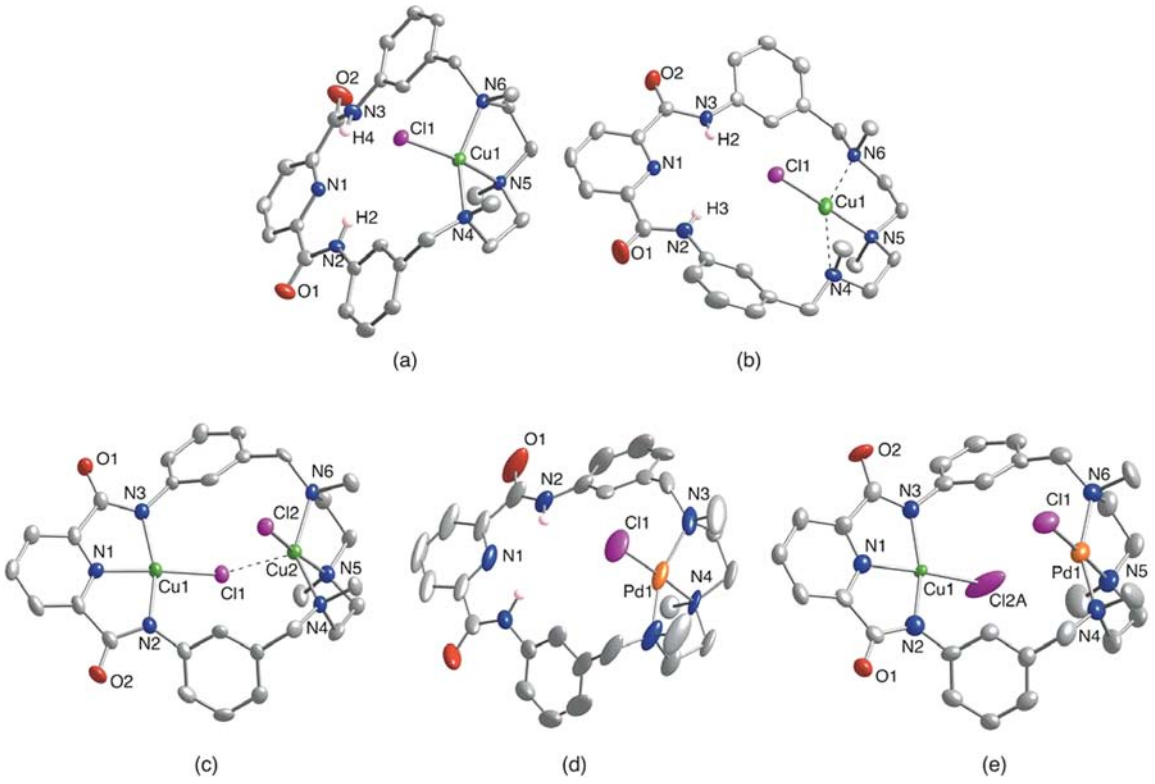

Figure 3. Representations of the X-ray crystals of (a) the cationic portion of $[(LH_2)CuCl]OTf$ (**4**), (b) $[(LH_2)CuCl]$ (**5**), (c) $[LCu_2Cl_2]$ (**7**), (d) the cationic portion of $[(LH_2)PdCl]Cl$ (**8**), and (e) $[LCuPdCl_2]$ (**10**) showing all non-hydrogen atoms (except the amide hydrogen atoms in **3**, **4**, and **8**) as 50% thermal ellipsoids.

trialkylamine unit [Cu1−N5 = 1.965(2) Å], with the other two at distances that indicate only weak interactions [2.847(2)−2.797(2) Å]. Thus, not surprisingly for Cu(I), the coordination geometry is essentially linear two-coordinate [N5−Cu−Cl1 = 178.12(7)°].

Addition of NaOMe to a blue solution of **4** in MeOH yielded a forest green solution, from which a green solid was isolated after filtration and removal of solvent. We hypothesize that this solid is best formulated as Na[LCuCl] (**6**, Scheme 1) on the basis of EPR and ESI-MS data; attempts to obtain crystals suitable for analysis by X-ray crystallography have not been successful. The EPR spectrum (Figure 2c,d) is significantly different from that of **4**, and features an axial signal with resolved hyperfine splitting to a single copper ion [$A_{\|}$(Cu) = 191 × 10^{-4} cm^{-1}] and three N atoms [$A_{\perp}(^{14}N)$ = 15 × 10^{-4} cm^{-1}] as determined by spectral simulation. Similar spectra have been reported for tetragonal complexes of ligand **3**,[13,14] consistent with binding of the copper ion in **6** to the pyridyldicarboxamide portion of the macrocycle. In addition, the negative ion ESI mass spectrum of **6** in MeOH exhibited a parent ion at m/z 582 with an isotope pattern consistent with $[\mathbf{6} - Na]^-$ (Figure S4; we were unable to observe a positive ion spectrum). Taken together, the data support the hypothesis that added base deprotonates the pyridyldicarboxamide portion of **4** and results in migration of the copper(II)−chloride moiety to this fragment to yield **6**.

Also consistent with the proposed formulation of **6** is that addition of $M^{II}Cl_2$ (M^{II} = Cu, Pd, or Pt) to **6** yielded dinuclear complexes **7**, **10**, and **11**. Compounds **7**, **10**, and **11** were fully characterized, with ESI-MS, CHN analysis, and X-ray crystallographic data being most informative. A peak envelope in the ESI mass spectrum for **7** is seen at m/z 705 with the appropriate isotope pattern for $[M + Na]^+$ (Figure S6). In the X-ray structure of **7** (Figure 3c), two Cu(II) ions are bound to the macrocycle 4.4847(13) Å apart. The coordination geometry for Cu1 is square planar, with metal−ligand distances similar to that in $[(\mathbf{3})CuCl]^-$.[13] Because chloride Cl1 weakly coordinates to Cu2 at a distance of 2.693(2) Å, the resulting coordination geometry for Cu2 is different than in **5** (τ = 0.28, where a value of 0 corresponds to square pyramidal and 1 denotes trigonal bipyramidal) and is best described as distorted square pyramidal (τ = 0.56) with Cl1 occupying the axial position.[26] The 2 K X-band EPR spectrum is broad and difficult to interpret without further detailed study (Figure S5).

The overall topologies of **10** (Figure 3e) and **11** (Figure S10) are similar to that of **7**, albeit with Pd(II) or Pt(II) instead of Cu(II) in the trialkyltriamine site. In contrast to **7** (τ = 0.56), the M(II) (M = Pd or Pt) geometries in **10** (τ = 0.35) and **11** (τ = 0.31) deviate little from square planar, and Cl2 does not interact significantly with the M(II) ion (Pd1···Cl2A and Pt1···Cl2b > 3.5 Å). This missing interaction accompanies Cu···Pd/Pt distances of 4.956(1) and 5.070(1) Å, respectively, for **10** and **11** that are ∼0.5 Å longer than the Cu···Cu separation in **7** (4.485(1) Å). These differences illustrate the ability of the supporting ligand to enable disparate metal−metal interactions. Consistent with their formulations, the EPR spectra of **10** and **11** exhibit similar axial signals with resolved hyperfine splitting to copper and nitrogen atoms (Figure S11 and S14; **10**, $g_{\|}$ = 2.197, $g_{\perp}$ = 2.053, $A_{\|}$(Cu) = 178 × 10^{-4} cm^{-1}, $A_{\perp}(^{14}N)$ = 13 × 10^{-4} cm^{-1}; **11**, $g_{\|}$ = 2.188, $g_{\perp}$ = 2.045, $A_{\|}$(Cu) = 178 × 10^{-4} cm^{-1}, $A_{\perp}(^{14}N)$ = 12 × 10^{-4} cm^{-1}). The complexes also exhibit peak envelopes in their ESI mass spectra with isotope patterns clearly attributable to heterodinuclear

dx.doi.org/10.1021/ic301914u | Inorg. Chem. 2013, 52, 793−799

Table 1. Selected Interatomic Distances (Å) and Angles (deg) for the Indicated X-ray Crystal Structures

[(LH$_2$)CuCl]OTf (**4**)			
Cu1−N4	2.058(4)	N5−Cu1−N4	85.83(16)
Cu1−N5	1.998(4)	N6−Cu1−N4	150.26(16)
Cu1−N6	2.043(4)	N5−Cu1−N6	86.12(16)
Cu1−Cl1	2.200(1)	Cl1−Cu1−N5	164.03(13)
		Cl1−Cu1−N4	97.37(12)
		Cl1−Cu1−N6	98.19(11)
[(LH$_2$)CuCl] (**5**)			
Cu1−N5	1.965(2)	N5−Cu1−Cl1	178.12(7)
Cu1−Cl1	2.136 (1)		
Cu1−N6	2.847(2)		
Cu1−N4	2.797(2)		
[LCu$_2$Cl$_2$] (**7**)			
Cu1−N1	1.911(6)	N1−Cu1−N2	80.0(3)
Cu1−N2	2.007(7)	N1−Cu1−N3	80.7(3)
Cu1−N3	1.999(6)	N2−Cu1−N3	158.9(3)
Cu1−Cl1	2.216(2)	N1−Cu1−Cl1	170.9(2)
Cu1···Cu2	4.484(1)	N2−Cu1−Cl1	100.29(19)
Cu2−N5	2.082(7)	N3−Cu1−Cl1	100.09(18)
Cu2−N6	2.097(7)	N5−Cu2−N6	85.1(3)
Cu2−N4	2.122(6)	N5−Cu2−N4	85.5(3)
Cu2−Cl2	2.241(2)	N6−Cu2−N4	139.8(2)
Cu2···Cl1	2.693(2)	N5−Cu2−Cl2	174.23(19)
Cu1···Cu2	4.4847(13)	N6−Cu2−Cl2	93.39(18)
		N4−Cu2−Cl2	92.08(18)
		N5−Cu2−Cl1	89.02(19)
		N6−Cu2−Cl1	109.27(17)
		N4−Cu2−Cl1	109.57(17)
		Cl2−Cu2−Cl1	96.72(7)
[(LH$_2$)PdCl]Cl (**8**)			
N4−Pd1	2.031(2)	N3−Pd1−N3A	159.8(3)
N3−Pd1	2.109(1)	N4−Pd1−N3	85.73(3)
Cl1−Pd1	2.286(1)	N4−Pd1−Cl1	174.98(2)
		N3−Pd1−Cl1	95.05(5)
[(LH$_2$)PtCl]Cl (**9**)			
N5−Pt1	2.0081(3)	N5−Pt1−N6	86.38(6)
N6−Pt1	2.080(1)	Cl1−Pt1−N5	175.38(1)
Cl1−Pt1	2.2998(3)	Cl1−Pt1−N6	94.24(1)
[LCuPdCl$_2$] (**10**)			
N1−Cu1	1.895(6)	Cl1−Pd1−N5	177.0(3)
N2−Cu1	1.977(8)	Cl1−Pd1−N6	94.3(2)
N3−Cu1	1.967(7)	Cl1−Pd1−N4	94.6(2)
N5−Pd1	2.081(7)	N5−Pd1−N6	86.3(3)
N6−Pd1	2.095(8)	N5−Pd1−N4	86.1(3)
N4−Pd1	2.086(8)	N6−Pd1−N4	155.6(3)
Pd1−Cl1	2.298(3)	Cl2B−Cu1−N3	99.0(3)
Cl2A-Cu1	2.095(10)	N3−Cu1−N2	158.4(3)
Cl2B−Cu1	2.314(16)	N3−Cu1−N1	81.3(3)
Pd1···Cu1	4.9561(9)	N2−Cu1−N1	79.6(3)
[LCuPtCl$_2$] (**11**)			
N5−Pt1	2.087(9)	N2−Cu1−Cl2B	98.7(4)
N1−Cu1	1.899(6)	N1−Cu1−Cl2B	178.7(5)
N2−Cu1	1.959(7)	Cl1−Pt1−N5	174.7(3)
Cl1−Pt1	2.284(3)		
Pt1···Cu1	5.070(1)		

CuPd and CuPt complexes (Figures 4, S12, and S13, respectively).

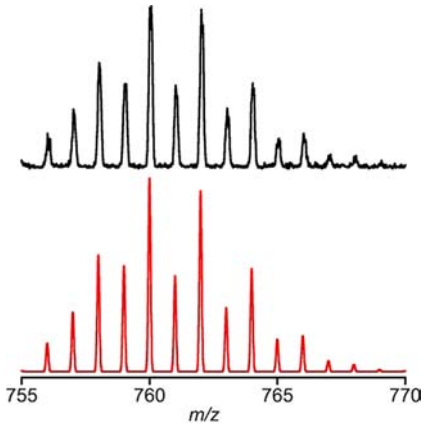

Figure 4. Negative ion ESI-MS peak envelope pattern for [M + Cl]$^-$ for **10** (top, black) and its simulation (bottom, red). The full spectrum is shown in Figure S12.

In addition to being accessible from addition of PdCl$_2$ to **6**, complex **10** can also be prepared from the monopalladium complex **8**, which is isolated by treating LH$_2$·2HCl with base and PdCl$_2$. An analogous complex **9** was prepared using PtCl$_2$ as starting material. The formulations of **8** and **9** are supported by ^{1}H NMR spectroscopy, CHN analysis, ESI-MS, and X-ray crystallography.[27] Notably, the ESI mass spectra contain parent ions with isotope patterns indicative of the presence of a single Pd or Pt atom (Figures S7 and S8). The X-ray crystal structures (Figure 3e for **8** and Figure S9 for **9**) are similar to that of **4**, with the exception of a Pd or Pt ion bound to the trialkyltriamine portion of the ligand instead of Cu(II). Addition of base and CuCl$_2$ to **8** generates **10**, illustrating how heterodinuclear complexes can be accessed by insertion of the different metal ions in either order (**6** + PdCl$_2$ or **8** + CuCl$_2$).

CONCLUSIONS

Ligand LH$_2$ serves as a versatile platform for the construction of a variety of mono- and dinuclear complexes comprising Cu, Pd, and Pt ions that have been thoroughly characterized by spectroscopy and X-ray crystallography. The ability to selectively insert Cu ions into either the pyridinedicarboxamide or trialkyltriamine portions of LH$_2$ is a unique feature, with the migration of Cu(II) from the latter to the former upon treatment with base being notable. Importantly, selective incorporation of divergent metal ions into the LH$_2$ frame yields new heterodinuclear Cu/Pd or Cu/Pt complexes that we envision will be useful for future reactivity studies, including ones aimed at understanding and developing new oxidation catalysts. The divergent supporting ligand environments in the dicopper complex **7** also are intriguing, for example, for developing new routes to dicopper−oxygen models of metalloenzyme active sites. With the coordination chemistry foundation now in hand, pursuit of new reactions promoted by disparate Cu$_2$, CuPd, and CuPt sites within the dinucleating ligand framework LH$_2$ can commence.

EXPERIMENTAL SECTION

General Procedures. All reactions and manipulations were performed under a pure argon atmosphere using Schlenk techniques or in a nitrogen atmosphere box unless otherwise noted. Solvents were passed through a solvent purification system (Glass Contour, Laguna CA) and degassed before use. Anhydrous grade *N,N*-dimethylforma-

dx.doi.org/10.1021/ic301914u | *Inorg. Chem.* 2013, 52, 793−799

mide (DMF) was purchased from Aldrich, degassed, and dried over activated 3 Å molecular sieves. Tetrahydrofuran (THF) was dried by reflux, under an argon atmosphere, over sodium metal with a benzophenone ketyl indicator and distilled prior to use. All chemicals were purchased from Aldrich and used without purification unless listed below. 3-*N*-Methylaminopentane-1,5-diamine was purchased from TCI Chemicals and used without further purification. Mesitylcopper(I) was prepared as described in the literature.[28] 1,3-*N,N″*-Di(3-nitrobenzyl)-*N,N′,N″*-trimethyldiethylenetriamine and LH_2·2HCl were prepared according a published procedure, except by using an alternate synthesis of intermediate 1,3-*N,N″*-di(3-aminobenzyl)-*N,N′,N″*-trimethyldiethylenetriamine (see below).[9c] All of the compounds except for Cu(I) complex **5** are air stable and appear to be stable in solution, as evinced by UV−vis and EPR spectroscopy.

Physical Methods. ^{1}H and $^{13}C\{^1H\}$ NMR spectra were recorded on a Varian VI-300 MHz spectrometer at ambient temperature. UV−vis spectra were collected on a HP8453 (190−1000 nm) diode array spectrophotometer. Electrospray ionization mass spectrometry (ESI-MS) was performed on a Bruker Bio-TOF II instrument. Elemental analyses were performed by Robertson Microlit Laboratory (Ledgewood, NJ). Infrared spectra were collected on a Nicolet Avatar 370 FT-IR equipped with a Smart OMNI Sampler. Perpendicular-mode X-band (9.62 GHz) EPR spectra were recorded on a Bruker Elexsys E500 spectrometer at 2 K. Simulations were performed using Bruker SimFonia software (version 1.25).

1,3-*N,N″*-Di(3-aminobenzyl)-1,3,5-*N,N′,N″*-trimethylethylenetriamine. To a solution of 1,3-*N,N″*-di(3-nitrobenzyl)-*N,N′,N″*-trimethyldiethylenetriamine (3.00 g, 7.23 mmol) in EtOH (150 mL) was added $SnCl_2$·$2H_2O$ (20 g, 89 mmol) and aqueous HCl (55 mL, 35%). The resulting suspension was heated in an oil bath to 80 °C after which stirring started. A clear solution formed within ∼5 min. The solution was refluxed for 12 h, during which precipitation of a white solid occurred. The suspension was allowed to cool to room temperature, and the solids were collected by filtration. The filtrate was concentrated to half of its original volume under reduced pressure, cooled for an hour in an ice bath, and the additional solid precipitate collected by filtration. The filtered solids were combined and washed with aqueous HCl (2 × 10 mL, 35%) and EtOH (2 × 20 mL) and dried *in vacuo* to obtain the product as a Sn_2Cl_{10}·2HCl adduct (5.50 g, 73%). IR (solid, cm^{-1}): 3070 (s), 3008 (s), 2900 (w), 2860 (vw), 1625 (w), 1568 (m), 1500 (s), 1492 (vs), 1392 (s), 1238(w), 1107 (m), 1016 (w), 988 (w), 965 (m), 942 (m), 897 (s), 795 (vs), 750 (s), 681 (vs). ^{1}H NMR (300 MHz, DMSO-d_6): δ 7.66 (d, J = 7.70 Hz, 2H), 7.54 (t, J = 7.70 Hz, 4H), 7.41 (d, J = 8.10 Hz, 2H), 4.45 (br, s, 4H), 3.59 (br. m, 8H), 2.75 (s, 3H), 2.69 (s, 6H) ppm. Anal. Calcd for $C_{21}H_{41}Cl_{12}N_5O_2Sn_2$ (Sn_2Cl_{10}·2HCl adduct + $2H_2O$): C, 23.83; H, 3.90; Cl, 40.19; N, 6.62; Sn, 22.43. Found: C, 23.43; H, 3.89; Cl, 40.83; N, 6.18; Sn, 21.20. The adduct (5 g, 4.9 mmol) in MeOH (50 mL) was slowly (5 min) added to a saturated methanolic solution of NaOH (20 mL) in a 250 mL beaker and stirred for 30 min. The mixture was filtered, and the filtrate was completely dried under reduced pressure, avoiding heating. The residue was mixed with Et_2O (20 mL) and filtered. The filtrate was dried *in vacuo* to yield the product as a light yellowish oil. This Et_2O extraction procedure was repeated until no residual solids were seen (1.04 g, 60% yield). The ^{1}H NMR data matched that reported previously.[9c]

[(LH$_2$)CuCl]OTf (**4**). A suspension of LH_2·2HCl (85 mg, 0.15 mmol) in THF (10 mL) was treated with a solution of sodium methoxide in methanol (0.70 mL, 0.35 mmol). Subsequent addition of a solution of $Cu(OTf)_2$ (54 mg, 0.15 mmol) in MeOH (2 mL) resulted in a deep blue mixture. The reaction mixture was stirred for 4 h and filtered, and the filtrate was evaporated to leave a blue-green solid. The solid was washed with isopropanol (2 × 5 mL) and dried *in vacuo* to yield the product as a blue solid (57 mg, 53%). X-ray quality crystals were obtained by slow evaporation of a solution of the complex in methanol solution at −20 °C. UV−vis (THF/DMF 2:1): λ_{max} (ε, M^{-1} cm^{-1}) 285 (∼11 000), 530 (∼200), 665 (∼140). ESI-MS (CH_3OH, m/z) calcd 584.17 (M-OTf), found 584.17. IR (solid, cm^{-1}): 1695 (s), 1681 (s), 1610 (m), 1552 (s), 1492 (s), 1438 (w), 1324 (w), 1263 (vs), 1222 (w), 1147 (m), 1035 (s), 1006 (w), 968 (w), 871 (w), 844 (s), 811 (s), 775 (s), 701 (m). EPR (9.64 GHz, toluene, 2 K): g_x = 2.170, g_y = 2.054, g_z = 2.034, $A_{\|}$(Cu) = 192 × 10^{-4} cm^{-1}. Despite repeated attempts, satisfactory CHN analysis results have not been obtained, which we hypothesize is due to the presence of salt coproducts in the blue solid that we were unable to fully separate.

[(LH$_2$)CuCl] (**5**). To a solution of LH_2·2HCl (50 mg, 0.09 mmol) in CH_2Cl_2 (3 mL) was added mesitylcopper(I) (56 mg, 0.3 mmol), and the mixture was stirred for 2 h. The mixture was then filtered, and Et_2O was allowed to slowly diffuse into the filtrate at −20 °C to yield the product as colorless crystals (23 mg, 0.04 mmol, 43% yields). UV−vis (DCM): λ_{max} (ε, M^{-1}cm^{-1}) 285 (∼12 000). IR (solid, cm^{-1}): 3315 (w), 2865 (w), 1683 (s), 1614 (s), 1589 (w), 1575 (w), 1542 (s), 1490 (s), 1450 (m), 1430 (m), 1370 (m), 1313 (m), 1265 (w), 1217 (w), 1180 (w), 1132 (w), 1047 (s), 1010 (w), 1000 (w), 983 (w), 950 (w), 904 (w), 883 (s), 842 (w), 832 (w), 781 (s), 731 (m), 670 (s), 670 (s). ^{1}H NMR (300 MHz, DMSO-d_6): δ 11.21 (s, 2H), 8.38 (br, 5H), 7.65 (s, 2H), 7.34 (t, J = 7.70 Hz, 2H), 7.01 (d, J = 7.00 Hz, 2H), 3.50 (s, 4H), 2.54 (br, s, 8H), 2.24 (br, s, 3H), 2.12 (br s, 6H). ESI-MS (CH_3OH) m/z (%): calcd 584.17 (M$^+$), found 584.12. Despite repeated attempts, satisfactory CHN analysis results have not been obtained, which we hypothesize is due to the presence of salt coproducts that we were unable to fully separate.

Na[LCuCl] (**6**). To a blue solution of **4** (50 mg, 0.068 mmol) in methanol (2 mL) was added 1.1 equiv of NaOMe (0.071 mL, 0.071 mmol, 1 M in methanol) to form a dark green mixture after 4 h stirring at room temperature. The mixture was filtered, and the solvent was removed. The residue was solved in THF (2 × 3 mL), filtered, and dried *in vacuo* to yield compound **6** as a green solid (32 mg, 80%). UV−vis (THF/DMF 2:1): λ_{max} (ε, M^{-1} cm^{-1}) 260 (∼6500 M^{-1} cm^{-1}), 662 (∼200 M^{-1} cm^{-1}). IR (solid, cm^{-1}): 2962 (w), 2860 (w), 2794 (w), 1610 (s), 1587 (s), 1575 (s), 1558 (m), 1538 (w), 1506 (w), 1484 (m), 1456 (m), 1434 (m), 1386 (m), 1375 (m), 1286 (s), 1260 (s), 1228 (m), 1164 (s), 1081 (w), 1037 (s), 1018 (w), 985 (w), 941 (w), 898 (w), 840 (w), 823 (w), 786 (w), 759 (s), 731 (w), 703 (m), 686 (s). ESI-MS (CH_3OH, m/z): calcd 582.15 [M − Na]$^-$, found 582.15. EPR (9.64 GHz, toluene, 2 K): $g_{\|}$ = 2.227, $g_{\perp}$ = 2.053, $A_{\|}$(Cu) = 191 × 10^{-4} cm^{-1}, $A_{\perp}$(^{14}N) = 15 × 10^{-4} cm^{-1}. Despite repeated attempts, satisfactory CHN analysis results have not been obtained, which we hypothesize is due to the presence of salt coproducts that we were unable to fully separate.

[LCu$_2$Cl$_2$] (**7**). To a solution of **6** (50 mg, 0.068 mmol) in DMF (1 mL) was added $CuCl_2$ (9.4 mg, 0.07 mmol) in MeOH (4 mL), the mixture was stirred for 12 h and filtered, and Et_2O was slowly diffused into the deep green filtrate over one week to afford the product as green crystals (18 mg, 37%). In an alternative, more direct method, compound **7** was synthesized by slow (10 min) addition of (2.2 equiv, 0.41 mmol) Bu_4NOH (1 M in MeOH) to the blue mixture of $CuCl_2$ (38 mg, 0.28 mmol) and LH_2 (70 mg, 0.14 mmol) in DMF (2 mL). The mixture stirred for 12 h, after which the solvent was removed *in vacuo* to yield a greenish powder. This powder was dissolved in CH_2Cl_2 and filtered, and solvent was removed from the filtrate. The product was then obtained in crystalline form via the slow evaporation of a MeOH solution of the product (20 mg, 41%). UV−vis (MeOH/DMF 3:1) λ_{max} (ε, M^{-1} cm^{-1}): 297 (6500 M^{-1} cm^{-1}), 632 (167 M^{-1} cm^{-1}). ESI-MS (CH_3OH, m/z): calcd 705.04 (M + Na), found 705.03. IR (solid, cm^{-1}): 2960 (w), 2923 (w), 2854 (vw), 1629 (s), 1618 (s), 1602 (w), 1589 (s), 1571 (s), 1486 (s), 1438 (m), 1375 (s), 1365 (vs), 1311 (w), 1159 (w), 1137 (w), 1076 (w), 1054 (w), 1039 (w), 997 (w), 962 (m), 952 (m), 939 (w), 904 (w), 839 (w), 812 (m), 770 (vs), 704 (m), 668 (m). EPR [9.64 GHz, MeOH/CH_2Cl_2 (1:7), 2 K]: $g_{\|}$ = 2.227, $g_{\perp}$ = 2.075, $A_{\|}$(Cu) = 173 × 10^{-4} cm^{-1}, $A_{\perp}$(^{14}N) = 19 × 10^{-4} cm^{-1}. Anal. Calcd for $C_{28}H_{32}Cl_2Cu_2N_6O_2$: C, 49.27; H, 4.73; N, 12.31. Found: C, 50.06; H, 4.73; N, 12.16.

[(LH$_2$)PdCl]Cl (**8**). A solution of $PdCl_2$ (41 mg, 0.24 mmol) in CH_3CN (5 mL) was added to a solution of LH_2·2HCl (100 mg, 0.22 mmol) and NEt_3 (46 mg, 0.044 mmol) in CH_3CN (5 mL). The mixture were stirred for 1 h and then warmed at 50 °C for 5 min. The yellow-brown mixture was filtered and Et_2O diffused slowly into the filtrate to afford the product as bright-yellow crystals (130 mg, 78%).

dx.doi.org/10.1021/ic301914u | *Inorg. Chem.* 2013, 52, 793−799

ESI-MS (CH_3OH, m/z): calcd 627.12 ($M^+ - Cl$), found 627.13. UV–vis (methanol) λ_{max} (ε, M^{-1} cm^{-1}): 230 (12 300), 281 (5700). IR (solid, cm^{-1}): 2958 (w), 2919 (w), 2850 (vw),1629 (s), 1618 (s), 1602 (w), 1590 (s), 1571 (s), 1484 (m), 1465 (w), 1438 (w), 1423 (vw), 1373 (s), 1363 (vs), 1315 (m), 1282 (vw), 1159 (vw), 1141 (w), 1076 (w), 1052 (w), 1039 (w), 997 (w), 966 (m), 952 (m), 937 (w), 906 (w), 836 (w), 811 (m), 768 (s), 755 (s), 702 (m), 686 (m). ^1H NMR (300 MHz, $CDCl_3$): δ 11.08 (br, s), 8.72 (d, J = 8.40 Hz, 2H), 8.39 (t, J = 8.80 Hz, 2H), 8.09 (s, 2H), 7.48 (t, J = 7.70 Hz, 2H), 7.10 (d, J = 7.30 Hz, 2H), 3.65 (s, 4H), 3.19 (m, J = 7.00 Hz, 8H), 2.47 (s, 6H), 2.03 (s, 3H). Anal. Calcd for $C_{28}H_{34}Cl_2N_6O_2Pd$: C, 50.65; H, 5.16; N, 12.66. Found: C, 49.86; H, 5.00; N, 12.30.

[(LH$_2$)PtCl]Cl (**9**). A solution of $PtCl_2$ (37 mg, 0.14 mmol) in DMSO (1 mL) was added to a solution of LH_2 (70 mg, 0.14 mmol) in DMSO (1 mL). The mixture was stirred for 4 h. The solvent was removed *in vacuo* and the residue washed with dry MeOH (2 × 2 mL) to yield the product as a yellowish solid (72 mg, 67%). X-ray quality crystals were obtained by slow evaporation of the complex in CH_2Cl_2. ESI-MS (CH_3OH, m/z): calcd 716.21 $(M - Cl)^+$, found 716.21, and calcd 794.22 $[(M + DMSO) - Cl)]^+$, found 794.20. IR (solid, cm^{-1}): 3500 (m), 3250 (m), 2960 (w), 2915 (w), 2855 (vw), 1681 (s), 1612 (s), 1552 (vs), 1492 (s), 1454 (m), 1330 (m), 1290 (w), 1263 (w), 1226 (w), 1172 (w), 1123 (w), 1027 (vs), 1000 (m), 950 (m), 883 (m), 840 (w), 815 (m), 800 (m), 790 (m), 763 (s), 746 (s), 701 (s), 682 (s). ^1H NMR (300 MHz, DMSO-d_6): δ 10.85 (s, 2H), 7.88 (d, J = 8.42 Hz, 2H), 7.57 (s, 2H), 7.50 (s, 2H), 6.64 (t, J = 7.92 Hz, 3H), 6.27 (d, J = 7.32 Hz, 2H), 3.52 (br, s, 8H), 2.69 (br, s, 6H), 2.60 (s, 3H), 2.58 (s, 6H). Anal. Calcd for $C_{28}H_{34}Cl_2N_6O_2Pt$ + (2DMSO): C, 42.29; H, 5.10; N, 9.25. Found: C, 42.52; H, 4.81; N, 9.52.

[LCuPdCl$_2$] (**10**). For method A, a solution of $PdCl_2$ (27 mg, 0.15 mmol) in CH_3CN (5 mL) was added to a solution of **6** (72 mg, 0.12 mmol) in DMF (2 mL). The resulting red-brown mixture was stirred overnight and then filtered. Solvent was removed from the filtrate, and the red residue was washed with sequentially with THF (2 × 2 mL) and Et_2O (2 mL) and then dried *in vacuo*. Slow evaporation from a solution in CH_3CN (5 mL) at 0 °C yielded **10** as purple crystals (28 mg, 32%). For method B, to a solution of **9** (70 mg, 0.1 mmol) in DMF (2 mL) was added 2.2 equiv of NaOMe (1 M in MeOH) or 2.2 equiv of $(^nBu)_4NOH$ (1 M in MeOH), and the mixture was stirred for 2 h. A solution of $CuCl_2$ (13.4 mg, 0.1 mmol) in MeOH (2 mL) was then added and the mixture stirred for an additional 12 h at room temperature. The mixture was filtered, and solvent was removed from the filtrate. The residue was washed with THF (2 × 3 mL) and dried *in vacuo* to yield the product as a brown-green solid (45 mg, 62%). X-ray quality purple crystals were grown by slow evaporation of a methanolic solution of the product. ESI-MS (CH_3OH, m/z): calcd 760.00 $(M + Cl)^-$, found 760.01. UV–vis (THF/DMF 3:1) λ_{max} (ε, M^{-1} cm^{-1}): 308 (6200), 587 (140). IR (solid, cm^{-1}): 2964 (w), 2919 (w), 2880 (vw), 1559 (s), 1575 (vs), 1488 (s), 1457 (m), 1436 (m), 1376 (s), 1313 (vw), 1268 (vw), 1162 (vw), 1141 (m), 1081 (w), 1041 (m), 951 (m), 900 (w), 881 (w), 819 (s), 771 (s), 760 (s), 703 (m), 680 (w), 668 (w). EPR (9.64 GHz, $CHCl_3$, 2 K): $g_{\|}$ = 2.197, $g_{\perp}$ = 2.053, $A_{\|}$(Cu) = 178 × 10^{-4} cm^{-1}, $A_{\perp}(^{14}N)$ = 13 × 10^{-4} cm^{-1}. Anal. Calcd for $C_{28}H_{32}Cl_2CuN_6O_2Pd$: C, 46.36; H, 4.45; N, 11.58. Found: C, 46.51; H, 4.33; N, 11.16 (note: the analysis sample was prepared by removing crystals manually from coprecipitated powdered material under a microscope).

[LCuPtCl$_2$] (**11**). For method A, a solution of $PtCl_2$ (37 mg, 0.14 mmol) in DMSO (1 mL) was added to a solution of LH_2 (70 mg, 0.14 mmol) in DMSO (1 mL). The mixture was stirred for 4 h, and to this was added 1.5 equiv of NaOMe (1 M in methanol) or 1.5 equiv of Bu_4NOH (1 M in methanol) and a solution of $CuCl_2$ (19 mg, 0.14 mmol) in DMSO (1 mL). The mixture was stirred for an additional 12 h at room temperature. Solvent was removed from the filtrate, and the green residue was washed sequentially with MeOH (2 × 2 mL). The solid was dissolved in CH_2Cl_2 (2 mL), filtered, and solvent removed from the filtrate *in vacuo* to yield the product (45 mg, 41%). X-ray quality single crystals formed upon the slow evaporation of a solution of **11** in CH_2Cl_2/MeOH (2 mL). For method B, a solution of $CuCl_2$ (19 mg, 0.14 mmol) in DMSO (1 mL) was added to a solution of LH_2 (70 mg, 0.14 mmol). The resulting blue solution was stirred for 1 h, and then 1.5 equiv of NaOMe or Bu_4NOH (1 M in methanol) was added to form a dark green mixture. A solution of $PtCl_2$ (37 mg, 0.14 mmol) in DMSO (1 mL) was added to the reaction mixture which was stirred for 12 h and then filtered. Solvent was removed from the filtrate, and the green residue was washed with MeOH (2 × 2 mL), filtered, and then solvent removed from the filtrate *in vacuo* to yield the product (34 mg, 32%). ESI-MS (CH_3OH, m/z): calcd 778.19 $(M - Cl)^+$, found 778.12. UV–vis (MeOH/DMF 1:1) λ_{max} (ε, M^{-1} cm^{-1}): 305 (8756), 598 (220). IR (solid, cm^{-1}): 2991 (w), 2957 (w), 1612 (s), 1578 (s), 1483 (m), 1429 (m), 1374 (s), 1313 (w), 1251 (s), 1143 (s), 1096 (s), 1028 (s), 933 (w), 843 (w), 803 (vs), 770 (s), 701 (w), 682 (s), 671 (m). EPR (9.64 GHz, CH_2Cl_2, 2 K): $g_{\|}$ = 2.188, $g_{\perp}$ = 2.045, $A_{\|}$(Cu) = 178 × 10^{-4} cm^{-1}, $A_{\perp}(^{14}N)$ = 12 × 10^{-4} cm^{-1}. Anal. Calcd for $C_{29}H_{36}Cl_2CuN_6O_3Pt$ (**10** + MeOH): C, 41.16; H, 4.29; N, 9.93. Found: C, 41.20; H, 4.10; N, 9.93.

■ ASSOCIATED CONTENT

Ⓢ Supporting Information

Spectroscopic data and descriptions of X-ray crystallographic data collections (PDF) and X-ray data (CIF). This material is available free of charge via the Internet at http://pubs.acs.org.

■ AUTHOR INFORMATION

Corresponding Author

*E-mail: wtolman@umn.edu.

Notes

The authors declare no competing financial interest.

■ ACKNOWLEDGMENTS

We thank the National Institutes of Health for financial support of this research (GM 47365) and Elizabeth Korsmo for her help with the preparation of compound **8**.

■ REFERENCES

(1) Mitic, N.; Smith, S. J.; Neves, A.; Guddat, L. W.; Gahan, L. R.; Schenk, G. *Chem. Rev.* **2006**, *106*, 3338–3363.

(2) (a) Tainer, J. A.; Getzoff, E. D.; Richardson, J. S.; Richardson, D. C. *Nature* **1983**, *306*, 284–287. (b) Fielden, E. M.; Rotilio, G. In *Copper Proteins and Copper Enzymes*; Lontie, R., Ed.; CRC Press, Inc.: Boca Raton, FL, 1984; Vol. *II*, pp 27–61.

(3) (a) Ferguson-Miller, S.; Babcock, G. T. *Chem. Rev.* **1996**, *96*, 2889–2907. (b) Michel, H.; Behr, J.; Harrenga, A.; Kannt, A. *Annu. Rev. Biophys. Biomol. Struct.* **1998**, *27*, 329–356.

(4) Takacs, J. M.; Jiang, X. *Curr. Org. Chem.* **2003**, *7*, 369–396.

(5) (a) Klinman, J. P. *Chem. Rev.* **1996**, *96*, 2541–2561. (b) Prigge, S. T.; Mains, R. E.; Eipper, B. A.; Amzel, L. M. *Cell. Mol. Life Sci.* **2000**, *57*, 1236–1259. (c) Culpepper, M. A.; Cutsail, G. E., III; Hoffman, B. M.; Rosenzweig, A. C. *J. Am. Chem. Soc.* **2012**, *134*, 7640–7643.

(6) Lindahl, P. A. *J. Inorg. Biochem.* **2012**, 172–178.

(7) See, for example: (a) Garcia-Bosch, I.; Ribas, X.; Costas, M. *Eur. J. Inorg. Chem.* **2011**, *2012*, 179–187. (b) Chufán, E.; Puiu, S.; Karlin, K. *Acc. Chem. Res.* **2007**, *40*, 563–572.

(8) (a) Gavrilova, A. L.; Bosnich, B. *Chem. Rev.* **2004**, *104*, 349–384. (b) Vigato, P. A.; Tamburini, S. *Coord. Chem. Rev.* **2004**, *248*, 1717–2128. (c) Sumby, C. J. *Coord. Chem. Rev.* **2011**, *255*, 1937–1967.

(9) Selected recent examples: (a) Golchoubian, H.; Rostami, L.; Kariuki, B. *Polyhedron* **2010**, *29*, 1525–1533. (b) Jarenmark, M.; Haukka, M.; Demeshko, S.; Tuczek, F.; Zuppiroli, L.; Meyer, F.; Nordlander, E. *Inorg. Chem.* **2011**, *50*, 3866–3887. (c) Huang, D.; Holm, R. H. *J. Am. Chem. Soc.* **2010**, *132*, 4693–4701.

(10) Himes, R. A.; Karlin, K. D. *Curr. Opin. Chem. Biol.* **2009**, *13*, 119–131.

(11) (a) Shiota, Y.; Yoshizawa, K. *Inorg. Chem.* **2009**, *48*, 838–845. (b) Yoshizawa, K.; Shiota, Y. *J. Am. Chem. Soc.* **2006**, *128*, 9873–9881.

(12) Balasubramanian, R.; Smith, S. M.; Rawat, S.; Yatsunyk, L. A.; Stemmler, T. L.; Rosenzweig, A. C. *Nature* **2010**, *465*, 115–119.

(13) Donoghue, P. J.; Tehranchi, J.; Cramer, C. J.; Sarangi, R.; Solomon, E. I.; Tolman, W. B. *J. Am. Chem. Soc.* **2011**, *133*, 17602−17605.
(14) Donoghue, P. J.; Gupta, A. K.; Boyce, D. W.; Cramer, C. J.; Tolman, W. B. *J. Am. Chem. Soc.* **2010**, *132*, 15869−15871.
(15) For example, see: (a) Mirica, L. M.; Ottenwaelder, X.; Stack, T. D. P. *Chem. Rev.* **2004**, *104*, 1013−1045. (b) Lewis, E. A.; Tolman, W. B. *Chem. Rev.* **2004**, *104*, 1047−1076. (c) Cole, A. P.; Mahadevan, V.; Mirica, L. M.; Ottenwaelder, X.; Stack, T. D. P. *Inorg. Chem.* **2005**, *44*, 7345−7364. (d) Mirica, L. M.; Rudd, D. J.; Vance, M. A.; Solomon, E. I.; Hodgson, K. O.; Hedman, B.; Stack, T. D. P. *J. Am. Chem. Soc.* **2006**, *128*, 2654−2665.
(16) (a) Hosokawa, T.; Takano, M.; Murahashi, S.-I. *J. Am. Chem. Soc.* **1996**, *118*, 3990−3991. (b) Hosokawa, T.; Nomura, T.; Murahashi, S.-I. *J. Organomet. Chem.* **1998**, *551*, 387−389.
(17) (a) Anderson, B. J.; Keith, J. A.; Sigman, M. S. *J. Am. Chem. Soc.* **2010**, *132*, 11872−11874. (b) Michel, B. W.; Steffens, L. D.; Sigman, M. S. *J. Am. Chem. Soc.* **2011**, *133*, 8317−8325.
(18) York, J. T.; Llobet, A.; Cramer, C. J.; Tolman, W. B. *J. Am. Chem. Soc.* **2007**, *129*, 7990−7999.
(19) Cornell, C. N.; Sigman, M. S. In *Activation of Small Molecules*; Tolman, W. B., Ed.; Wiley-VCH: Weinheim, 2006, pp 159−186.
(20) Boisvert, L.; Goldberg, K. I. *Acc. Chem. Res.* **2012**, *45*, 899−910.
(21) Khusnutdinova, J. R.; Rath, N. P.; Mirica, L. M. *Angew. Chem., Int. Ed.* **2011**, *50*, 5532−5536.
(22) Khusnutdinova, J. R.; Qu, F.; Zhang, Y.; Rath, N. P.; Mirica, L. M. *Organometallics* **2012**, *31*, 4627−4630.
(23) Mueller, J. A.; Cowell, A.; Chandler, B. D.; Sigman, M. S. *J. Am. Chem. Soc.* **2005**, *127*, 14817−14824.
(24) Mitsudome, T.; Mizumoto, K.; Mizugaki, T.; Jitsukawa, K.; Kaneda, K. *Angew. Chem., Int. Ed.* **2009**, *49*, 1238−1240.
(25) While this paper was under review, a publication appeared describing some heterobimetallic complexes of L^{2-} and related ligands: Zhang, X.; Huang, D.; Chen, Y.-S.; Holm, R. H. *Inorg. Chem.* **2012**, *51*, 11017−11029.
(26) Addison, A. W.; Rao, T. N.; Reedijk, J.; van Rijn, J.; Verschoor, G. C. *J. Chem. Soc., Dalton Trans.* **1984**, *7*, 1349−1356.
(27) In the structure of **8**, Cl2 is disordered, and was modeled in two positions at 49% and 51% occupancy each (Cl2A and Cl2B). See the Supporting Information for details.
(28) Tsuda, T.; Yazawa, T.; Watanabe, K.; Fujii, T.; Saegusa, T. *J. Org. Chem.* **1981**, *46*, 192−194.